Deformation-Induced Injury of Alveolar Epithelial Cells
Effect of Frequency, Duration, and Amplitude

DANIEL J. TSCHUMPERLIN, JANE OSWARI, AND SUSAN S. MARGULIES

Department of Bioengineering, University of Pennsylvania, Philadelphia, Pennsylvania

The onset of ventilator-induced lung injury (VILI) is linked to a number of possible mechanisms. To isolate the possible role of alveolar epithelial deformation in the development of VILI, we have developed an *in vitro* system in which changes in alveolar epithelial cell viability can be measured after exposure to tightly controlled and physiologically relevant deformations. We report here a study of the relative effect of deformation frequency, duration, and amplitude on cell viability. We exposed rat primary alveolar epithelial cells to a variety of biaxial stretch protocols, and assessed deformation-induced cell injury quantitatively, using a fluorescent cell viability assay. Deformation-induced injury was found to depend on repetitive stretching, with cyclic deformations significantly more damaging than tonically held deformations. In cyclically deformed cells, injury occurred rapidly, with the majority of cell death occurring during the first 5 min of deformation. Deformation-induced injury was increased with the frequency of sustained cyclic deformations, but was not dependent on the deformation rate during a single stretch. Reducing the amplitude of cell deformations by superimposing small cyclic deformations on a tonic deformation significantly reduced cell death as compared with large-amplitude deformations with the same peak deformation.

Ventilator-induced lung injury (VILI) is a growing concern in the management of mechanically ventilated patients (1, 2). The onset of VILI in animal and isolated lung models has been ascribed to several possible mechanisms, including repeated collapse and reopening of air spaces (3), inflammation and neutrophil influx (4), changes in hemodynamic pressures (5), surfactant inactivation (6), and injurious deformations of the cellular constituents of the lung (7). One of the hallmarks of severe VILI is the presence of alveolar edema (1), presumably due to breakdown of the blood–gas barrier. The alveolar epithelium forms a continuous lining of the alveolar air spaces of the lung, provides the majority of resistance to fluid and protein transport between the vasculature and air space (8), and facilitates the efficient clearance of alveolar edema in response to injury (9). We have previously shown that the basement membrane underlying the alveolar epithelium expands as lung volume approaches physiologic limits (10), suggesting that the alveolar epithelium may be exposed to large deformations during ventilation to high lung volumes. Primary mechanical injury of the alveolar epithelium may thus be one of the initiating mechanisms associated with VILI.

Supporting this hypothesis has been the demonstration of changes in the alveolar epithelial barrier associated with lung inflation in a variety of preparations and with various measurement techniques. Ventilator studies with animals have shown that epithelial injury, as measured by electron microscopy and the presence of alveolar edema, depends on lung volume rather than on pressure (7, 11). In fluid-filled isolated lungs undergoing static inflation (12–15), epithelial permeability to a variety of tracers of different molecular weights increases slightly with increasing lung volume until large-scale breaks occur in the epithelial barrier. Electron microscopy has shown that the alveolar epithelium exhibits an increasing frequency of breaks when fixed at increasing lung volumes (16). In earlier *in vitro* work, we demonstrated that primary alveolar epithelial cells were increasingly vulnerable to cell death when deformations exceeded those associated with inflation to TLC (17).

Despite these advances, the relative importance of end-expiratory volume, end-inspiratory volume, and tidal volume (V_T) in the development of VILI remains controversial (1–3, 18), and uncertainty about the relative importance of these volumes continues to hinder the development of ventilator settings and strategies intended to limit VILI. Ideally, end-expiratory, end-inspiratory volume, and V_T should be varied independently to determine their relative importance in the development of VILI. In practice, it is rare that these volumes can be changed without alterations in other potentially important parameters (e.g., inspired oxygen fraction, flow waveform, and respiratory frequency and duration), each of which may effect lung injury independent of changes in lung volume (1). Furthermore, changes in the lung volume cycling protocol can introduce changes in surfactant activity, airway opening and collapse, hemodynamics, and blood gas exchange, all of which may have independent effects on epithelial integrity.

To isolate the role of alveolar epithelial deformation in the development of VILI, we have developed an *in vitro* system in which changes in alveolar epithelial cell viability can be measured after exposure to tightly controlled and physiologically relevant cyclic deformations (17). In the study reported here, we exposed rat primary alveolar epithelial type II (ATII) cells to a variety of deformation protocols with the goal of identifying the relative importance of deformation frequency, duration, and amplitude in deformation-induced cell injury. Our primary finding was that cell death can be reduced by limiting the amplitude of deformation, even while peak deformations are kept constant. This result suggests that ventilator strategies that limit changes in V_T and the concomitant epithelial deformations may limit epithelial injury during mechanical ventilation.

METHODS

Cell Culture Protocol

ATII cells were isolated from specific-pathogen–free male Sprague–Dawley rats (Harlan Sprague–Dawley, Indianapolis, IN) weighing 180 to 200 g. Rats were anesthetized with pentobarbital sodium (50 mg/kg body weight, intraperitoneally). After the trachea was cannulated, the lungs were mechanically ventilated, an abdominal aortotomy was performed, and the lungs were perfused via the pulmonary artery to remove blood. The lungs were then excised, and ATII cells were dissociated and isolated in a technique adapted from Dobbs and coworkers (19). Elastase solution (7 ml, 3 U/ml; Worthington Biochemical, Lakewood, NJ) was instilled into the airways of the excised lungs and incubated for 32 min, with an additional 6 ml instilled at 12

(*Received in original form July 2, 1998 and in revised form November 22, 1999*)

Supported by grant HL57204 from the National Institutes of Health, grant BES-9702088 from the National Science Foundation, and the Whitaker Foundation.

Dr. Tschumperlin was supported by a Whitaker Graduate Fellowship.

Correspondence and requests for reprints should be addressed to Susan Margulies, Department of Bioengineering, 3320 Smith Walk, Philadelphia, PA 19104-6392. E-mail: margulies@seas.upenn.edu

and 22 min of incubation. The lungs were then finely minced in the presence of deoxyribonuclease (Sigma Chemicals, St. Louis, MO), using a tissue chopper. The elastase reaction was stopped with fetal bovine serum (FBS; GIBCO BRL/Life Technologies, Gaithersburg, MD). Cells were purified by filtration and plating on bacteriologic plastic plates precoated with rat IgG (Sigma), using 3 mg IgG in 5 ml Tris-HCl per plate. After 1 h of incubation, the type ATII cells were isolated from the macrophages and contaminating cells by "panning" (19). Cell purity was assessed by phosphine 3R staining of adherent cells at 24 h, and was > 95% (20).

ATII cells were resuspended in minimum essential medium with Earle's salts and L-glutamine (Mediatech; Fisher Scientific, Pittsburgh, PA), supplemented with 10% FBS and penicillin (100 U/ml) and streptomycin (0.1 μg/ml) (all from GIBCO BRL/Life Technologies). Cells were plated at 1.0×10^6 cells/cm^2 on silastic membranes coated with fibronectin (40 μg/ml; Boehringer Mannheim Biochemicals, Indianapolis, IN). Cell attachment was limited to the central portion of each custom-made well by placing a piece of Tygon tubing in the center of each well and seeding cells only within this restricted area. Cells were incubated in 5% CO_2 at 37° C, with the cell medium replaced every 24 h, and were studied at 5 d after isolation. At this time the cells have attained some morphologic and phenotypic characteristics of type I alveolar epithelial cells (21–23), and have a greatly increased resistance to deformation-induced injury (17). Because our primary objective in the present study was to investigate the effect of deformation on integrity of the blood–gas barrier, which is lined primarily by type I cells, we focused our attention on cells after 5 d in culture.

Cell Deformation Protocol

The custom-designed device that we used for cell deformation studies is described in detail elsewhere (17). Briefly, wells are formed by securing a 0.2-mm–thick silicone membrane (gloss/gloss finish; Specialty Manufacturing, Saginaw, MI) to the bottom of a custom-designed polysulfone ring with a rubber o-ring pressed into a groove in the bottom of each polysulfone ring. When the cells are to be deformed, up to nine wells are mounted in the cell-stretching device, on a stationary top plate. Membrane deformation is provided by annular indentors that contact the bottom of each silicone membrane near the periphery of the cell culture surface. Simultaneous vertical displacement of each indentor results in sliding of the membrane over the indentor surface and stretching of the membrane in the plane transverse to the direction of indentor motion. Indentor motion is provided by a variable-speed DC motor (Bodine Electric, Chicago, IL), with minimum stretch and stretch amplitude set independently with a cam and linkage that connect the motor to the indentor assembly.

A schematic illustration of the various deformation protocols is shown in Figure 1. To investigate the effect of static deformation on cell viability, we mounted one or two wells each, from three separate cell isolations, in the deformation device and adjusted the conditions (~ 6%/s) until membrane surface area (SA) was increased by 25%, 37%, or 50%. The static deformations were then held for 1 h. These deformations were selected on the basis of a previously derived relationship between epithelial basement membrane SA and lung volume in isolated rat lungs (10 [Table 2 and Figure 3a]). The equation derived from these data is:

$$\%\Delta SA = 0.0057 \cdot (\%TLC)^2 - 0.2608 \cdot (\%TLC) + 4.8021$$

The chosen deformations are roughly equivalent to the change in epithelial basement membrane SA between RV and 80%, 100%, and > 100% TLC. To study the influence of deformation rate, we exposed three wells from three separate isolations to a single deformation of 50% ΔSA over periods of either 4 s or 1 s. To separate the effect of deformation frequency from the cumulative number of cyclic deformations, we exposed two to three wells from three separate isolations to 50% ΔSA at 15 cyles/min (cpm) for 60 min, or to 60 cpm for 15 min (a total of 900 deformation cycles for both). To examine the early time course of cell injury in cyclically deformed wells, we exposed three or four wells from each of four cell isolations to either 5 min or 60 min of 50% ΔSA at 15 cpm. To examine the effect of an extended duration of cyclic deformation on cell viability, we subjected two or three wells from three separate cell isolations to cyclic deformations of 25% ΔSA for 6 h at 15 cpm. To investigate the relative importance of minimum and maximum deformation and deformation amplitude, we statically deformed one or two wells from an additional three cell isolations as in the manner described earlier until membrane deformations (ΔSA) reached 25%, and then subjected them to 1 h of cyclic deformation (15 cpm) of 12% or 25%, resulting in peak deformations of 37% and 50% ΔSA, respectively. One or two wells from each isolation were included in each protocol as unstretched controls.

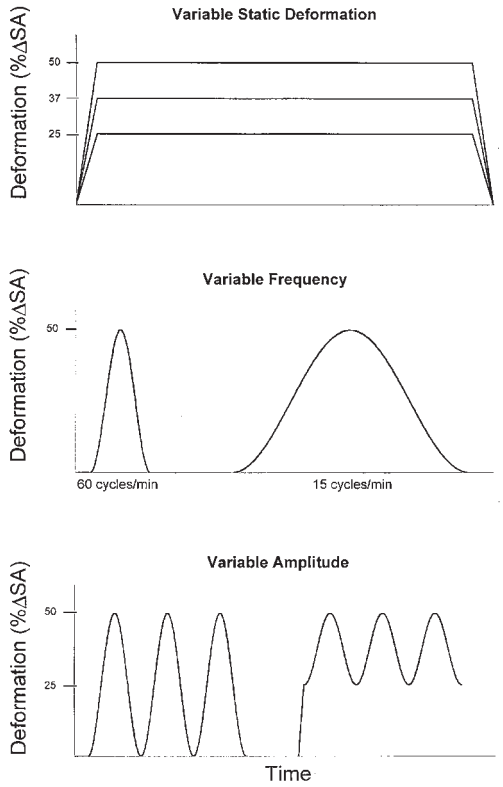

Figure 1. Schematic representation of the various deformation protocols used in the study. Static protocols were achieved by ramping up deformation (~ 6%/s) until the desired deformation level was reached. Deformations were held for 60 min and then released (~ 6%/s). The effect of frequency was determined by exposing cells either to a single sinusoidal deformation cycle (50% ΔSA) over either 1 s (60 cpm) or 4 s (15 cpm), or to an identical number of cycles (900) at 15 cpm and 60 cpm (not shown). The relative importance of deformation magnitude and amplitude were tested by exposing cells to cyclic deformations of matched magnitude (50% ΔSA in the case illustrated here) with different amplitudes (either 50% ΔSA or 25% ΔSA).

Measurement of Cell Injury

Before the wells were placed in the cell stretching device, each was washed three times with phenol red and serum-free Dulbecco's minimum essential medium supplemented with penicillin (100 U/ml) and streptomycin (0.1 mg/ml) (all from GIBCO BRL/Life Technologies), in which sodium bicarbonate was replaced with 20 mM 4-(2-hydroxyethyl)-1-piperazine-*N*-2-ethanesulfonic acid. The experiments were conducted at 37° C in room air (with the exception of the 6-h experiments, which were conducted in 5% CO_2 with the bicarbonate-buffered medium). To evaluate cell viability, we added ethidium homodimer-1 and calcein AM to wells to final concentrations of 0.23 μM 0.12 μM, respectively (Live/Dead Kit; Molecular Probes, Eugene, OR). Ethidium homodimer-1 (excitation/emission: ~ 495 nm/~ 635 nm), which is excluded by the intact plasma membrane of live cells, enters cells with damaged membranes and undergoes a fluorescence enhancement on binding to nucleic acids. Calcein AM (excitation/emission: ~ 495 nm/~ 515 nm, respectively) is well retained within living cells. Fluorescent dyes were added at the onset of stretching for the 1 h, 5 min, and one-stretch protocols, and at 1 h before the conclusion of the 6-h protocol, with microscopic visualization carried out 1 h af-

ter addition of the dyes in all cases. In previous work, we found no difference between adding the fluorescent dyes before or after the stretching protocol (17). Wells were examined with an inverted epifluorescence microscope (Diaphot; Nikon), with images of cells captured and stored with a digital imaging system (Hamamatsu CCD camera and controller; Metamorph 2.5, Universal Imaging, West Chester, PA). Images were acquired randomly from four locations in each well, with a ×20 objective, using separate filter blocks for visualization of ethidium homodimer-1 and calcein AM. Two images from each well were subsequently analyzed by counting of stained cells, and the percentage of dead cells was determined. The fraction of dead cells in unstretched control wells (always $< 1\%$) was subtracted from the fraction of dead cells found in stretched wells, thus the reported percentage of dead cells reflects cell death that is attributable to the deformation protocol.

Data Analysis

Results are presented as mean ± SD. Multiple observations from each well were averaged and counted as a single experimental measurement. Data were compared by analysis of variance with the JMP statistical package (SAS Institute, Cary, NC). Differences were regarded as statistically significant when $p < 0.05$.

RESULTS

Previously, we demonstrated that deformation-induced injury of alveolar epithelial cells was significantly greater when cyclic deformation was continued for 60 min (at 15 cpm) than with a single deformation at the same frequency. In the present study, to determine whether the increasing damage was due to the duration of the deformation protocol or to the repetitive nature of the cyclic protocol, we applied a single deformation that was held for 60 min (static). As in the cyclic studies, cell death increased nonlinearly with static deformation, rising dramatically at deformations of static ΔSA to 50% ΔSA (Figure 2), which corresponds roughly to lung inflation to a volume greater than TLC (10). Although the cell death caused by a 1-h static deformation was statistically indistinguishable from that caused by a single cycle (1 stretch) occurring over a period of ~ 4 s, deformation-induced cell death was significantly lower at each deformation magnitude in the static groups than with cells exposed to cyclic deformation (15 cpm) for an identical duration (Figure 2) (17). This finding indicates that cell injury depends not so much on the duration of deformation as on the repetitive nature of cell deformations.

We next performed experiments to examine whether deformation-induced injury was dependent on the frequency of deformation. With a device similar to that used on our study, cell injury in astrocytes has been found to depend on the rate of deformation, although at much higher rates than used in our study (24). Because of limitations of our deformation device, the highest frequency we could apply was 60 cpm. Because cell death depends on the number of deformation cycles, we first chose to apply a single deformation of 50% ΔSA at either 15 cpm or 60 cpm. Although there was a small increase in the percentage of dead cells when the rate was quadrupled, this did not reach statistical significance (Figure 3). To more fully study the effect of deformation frequency, we exposed cells to an identical number of deformation cycles (900 cycles, 50% ΔSA) at either 15 cpm or 60 cpm. The effect of frequency in this case was highly significant ($p < 0.05$). Thus, the data suggest that for the deformation rate to exert a significant effect on cell injury, rapid deformation cycling must be sustained.

To gain insight into the time course of repetitive-deformation–induced injury, we next performed experiments at times shorter and longer than the 60-min duration we had previously examined. There was no difference in deformation-induced injury when 25% ΔSA cyclic deformation was continued beyond 1 h for a total of 6 h (Figure 4), suggesting that continued cyclic deformation beyond 1 h did not increase damage to the cell layer. We therefore focused our attention on the development of injury between a single deformation and 1 h of sustained cycling. As can be seen in Figure 4, more than two-thirds of the observed deformation induced injury occurred within the first 5 min of cyclic stress. Thus, although we had earlier shown that injury was dependent on the repetitive nature of deformation, this effect appeared to diminish with sustained cycling.

The significant increases in cell death with increasing static deformation (Figure 2), and increasing dynamic deformation (17) clearly indicate that maximum deformation plays a role in deformation-induced cell injury. To investigate the relative importance of peak deformation magnitude and cyclic deformation amplitude on deformation-induced injury, we subjected cells to cyclic deformation amplitudes of 12% ΔSA and 25% ΔSA superimposed on a static deformation of 25% ΔSA, resulting in peak deformation magnitudes of 37% ΔSA and 50% ΔSA (Figure 1). (Here we define peak magnitude as the maximum deformation achieved above the resting state, in analogy to end-inspiratory volume, whereas amplitude is used to denote the amount of cyclic deformation, in analogy to V_T.) Restricting data analysis to these deformation protocols and the cyclic deformation protocols described previously (17), we found that deformation-induced injury did not depend on minimum deformation, but did vary significantly with both peak magnitude and deformation amplitude. The most intriguing finding in these studies was that limiting the deformation amplitude resulted in significant reductions in deformation-induced cell death at identical peak deformations (Figure 5). Thus, al-

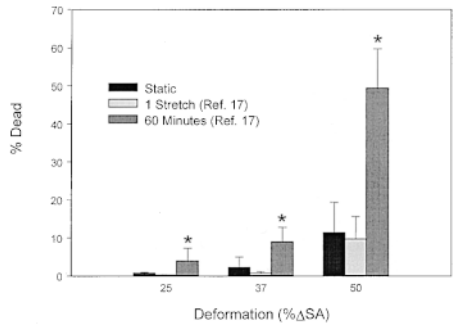

Figure 2. Comparison of 1-h static deformation with previously reported (17) single deformation and 1-h cyclic deformation (15 cpm). Data are presented as mean ± SD. Although the percentages of dead cells associated with single and static deformations were not significantly different from each other at any deformation level, both static and single deformations were significantly less injurious than were cyclic deformations at each deformation level. *$p < 0.05$.

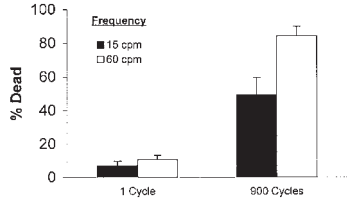

Figure 3. Dependence of deformation-induced cell death on deformation frequency. *Left*: cells were exposed to a single deformation (50% ΔSA) applied over a period of either ~ 4 s (*closed rectangles*: 15 cpm) or ~ 1 s (*open rectangles*: 60 cpm). Data are not significantly for the two different conditions ($p > 0.05$) *Right*: cells were exposed to an identical number of deformation cycles (900) at either 15 cpm or 60 cpm, again using 50% ΔSA. Cell death in this case was significantly dependent on frequency ($p < 0.05$).

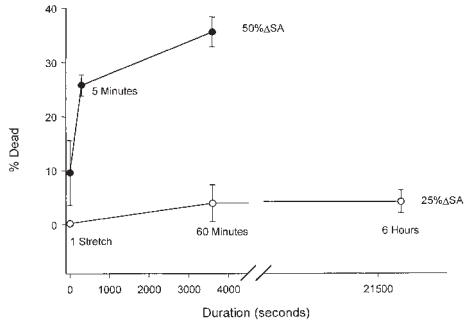

Figure 4. Development of deformation-induced cell death over time for 25% ΔSA and 50% ΔSA. Note break in time axis between 1-h and 6-h time points.

though cell death increases with the magnitude of cell deformation, this effect can be mitigated by increasing the minimum deformation while reducing the amplitude of deformation.

DISCUSSION

The results presented here show that the primary determinants of deformation-induced cell death are the amplitude and magnitude of deformation and the number and frequency of cyclic changes in cell SA. Although our earlier work demonstrated the general concept that repetitive cyclic deformations were more damaging to cells than was a single deformation, the results presented here emphasize that the deleterious effects of repetitive cycling are most severe in the first few minutes of cycling, with little additional cytotoxicity beyond 1 h of cycling.

The most intriguing finding of these studies was the diminution of cell death when deformation amplitude was reduced, even when peak deformation was maintained. As reported by Dreyfuss and Saumon in a recent review (1), a wealth of experimental evidence supports the concept that ventilation with positive end-expiratory pressure (PEEP) and reduced V_T is less injurious than ventilation with zero end-expiratory pressure and a higher V_T for the same peak airway pressure. The postulated explanations for this improved outcome include preservation of surfactant function (6), changes in cardiac output and hemodynamic pressures (5), and prevention of repeated recruitment and collapse of alveoli (3), which may produce large shear stresses on the epithelial layer. Our *in vitro* findings suggest that an additional benefit of limiting V_T is the resulting reduction in epithelial deformation amplitude, which may help to preserve cell viability and the integrity of the alveolar epithelial barrier.

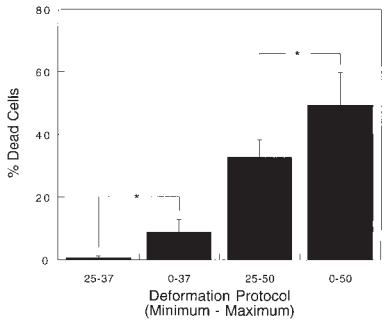

Figure 5. Relative importance of deformation magnitude and amplitude. Deformations were applied for 60 min, at 15 cpm. Data are given as mean ± SD. Reducing the amplitude to 12% ΔSA or 25% ΔSA significantly reduced cell death when maximum deformation was held at 37% ΔSA or 50% ΔSA, respectively. *$p < 0.05$.

Limitations

Before discussing the implications of our *in vitro* findings for mechanical ventilation of human lungs in the clinical setting, it is necessary to discuss several limitations of the present study. As discussed in detail elsewhere (21–23), ATII epithelial cells undergo major morphologic and phenotypic changes over the first few days in culture. By 5 d in culture the cells have a severely reduced ability to secrete surfactant, and express many of the phenotypic markers of alveolar epithelial type I cells, the cell type that covers the great majority of the alveolar surface (> 90%) (25). In addition, we have previously shown that by 5 d in culture these cells exhibit a greatly increased resistance to deformation-induced cell death (17). In the absence of a readily available alternative for examining the cellular physiology of the alveolar epithelial barrier (21), alveolar epithelial cells maintained in culture for several days have been used extensively to characterize the active and passive transport properties of this monolayer (26). Despite the limitations inherent in this primary cell culture preparation (21), it is interesting to note the close correspondence between the occurrence of alveolar epithelial type I cell injury in electron micrographs of rat lungs exposed to inflations beyond TLC (11) and the dramatic increase in deformation-induced injury that occurs in primary cultures of alveolar epithelial cells when deformations exceed those associated with inflation to TLC.

Although the present study focused primarily on changes in cell viability over a period of 1 h of deformation, there is evidence in the literature that significant injury can develop over longer time periods at more moderate pressures (27). Our results indicate that *in vitro*, cell injury does not increase significantly between 1 and 6 h of continuous cyclic deformation (Figure 4). It therefore seems likely that the development of injury over longer periods in normal animals involves other mechanisms of injury.

The primary goal of this study was to investigate the deleterious effects of deformation on alveolar epithelial viability. The advantage of this experimental approach is the ability to remove other possible injurious factors, thus better establishing the mechanisms and deformations specifically associated with deformation-induced injury. Additional factors associated with alveolar epithelial injury, including high concentrations of O_2 (28), can be included in future studies to address the possibility that these agents act synergistically with deformation to increase cellular injury.

Of further importance is that the outcome measure of the present and related studies is the breakdown of cell membrane integrity, which leads to cell death. This outcome measure is at the extreme end of what is most likely a spectrum of deformation-induced changes in cell physiology (3, 29–31). Some of these changes may be protective for the cell, but others are probably representative of more subtle forms of injury, resulting in the failure of cells to exercise their normal functions. These latter changes may be manifested in a number of ways, including increased leakiness of the tight junctions connecting alveolar epithelial cells (32) or changes in active transport across the alveolar epithelial barrier (33). A more sophisticated understanding of acute and chronic responses of the alveolar epithelium to deformation will be gained by examining these and other more subtle changes in cell physiology.

Implications for Clinical Mechanical Ventilation

Despite the limitations of the *in vitro* preparation used in our study, the results of the study raise several issues of impor-

tance for mechanical ventilation in the clinical setting. It is clear from the results presented here, and those presented previously (17), that deformation of the alveolar epithelium can lead to significant changes in cell viability. Although these findings do not rule out the possible importance of other mechanisms associated with ventilator-induced lung injury, the results of this study emphasize the need to consider the cell deformations that accompany mechanical ventilation in selecting ventilator settings and strategies. Although the current results, and those with healthy animal lungs (1), show that alveolar epithelial injury is modest when deformations are less than those associated with TLC, the extension of these findings to the diseased lung is less clear (34, 35). This may especially apply to disorders such as acute respiratory distress syndrome, in which computed tomography demonstrates that increased edema fluid leads to overexpansion of some alveoli while others remain closed or flooded (36, 37).

The administration of PEEP is now used widely in the ventilation of patients with acute lung injury, with several postulated rationales for improved lung function (2). In animal ventilation studies, the application of PEEP with end-inspiratory lung volume kept constant is always less injurious than for ventilation at a large V_T in the absence of PEEP (1). Because alveolar epithelial injury was mitigated by reducing the amplitude of cyclic deformations, our *in vitro* results suggest that one advantage of concurrently limiting end-inspiratory lung volume and reducing V_T is reduced injury of the alveolar epithelium. In addition, we have shown that large static increases in SA are much less damaging than cyclic increases in SA of the same magnitude, indicating that epithelial viability is not adversely affected by the application of large static deformations associated with PEEP at volumes up to TLC. Moreover, the dependence of alveolar epithelial injury on repetitive rather than on single changes in SA indicates that the use of occasional deep inspirations to recruit collapsed alveoli should not have a serious negative impact on alveolar epithelial viability.

The application of these *in vitro* findings to the much more complex *in vivo* situation requires great care, since changes in surfactant, hemodynamics, and blood gas may all contribute either positively or negatively to the preservation of lung function (1, 18). Nevertheless, the results of this study show that ventilation strategies such as the "open lung approach" with permissive hypercapnia (38), and high-frequency ventilation (2), both of which increase the mean airway pressure while limiting end-inspiratory lung volume and reducing V_T, should be very effective in preserving epithelial viability, which is critical to gas exchange and the resolution of alveolar edema (9). Although our *in vitro* results suggest that frequency is a major determinant of deformation-induced cell damage, it is not clear how this dependence would translate to the clinical application of high-frequency ventilation, in which the amplitudes of cell deformations are likely to be much smaller than even the smallest deformations used in the present study. This is an issue that deserves further study.

Conclusions

We used a previously developed experimental model of *in vitro* deformation of the alveolar epithelium to show that deformation-induced injury of this alveolar epithelium can be reduced by limiting the magnitude and amplitude of deformation or by limiting the repetitive changes in SA. Although care must be taken in extrapolating these results to the complex environment of the heterogeneously injured and inflated human lung, these results indicate that alveolar epithelial integrity should be protected by ventilation strategies that limit end-inspiratory lung volume and V_T. Although deformation of the alveolar epithelium is only one of many factors to consider in the application of mechanical ventilation, the results of this study indicate the important role of mechanical factors in determining alveolar epithelial viability and the integrity of the blood-gas barrier.

References

1. Dreyfuss, D., and G. Saumon. 1998. Ventilator–induced lung injury: lessons from experimental studies. *Am. J. Respir. Crit. Care Med.* 157:294–323.
2. Marini, J. J. 1996. Evolving concepts in the ventilatory management of acute respiratory distress syndrome. *Clin. Chest Med.* 17:555–575.
3. Tremblay, L., F. Valenza, S. P. Ribeiro, J. Li, and A. S. Slutsky. 1997. Injurious ventilatory strategies increase cytokines and c-fos mRNA expression in an isolated rat lung model. *J. Clin. Invest.* 99:944–952.
4. Kawano, T., S. Mori, M. Cybulsky, R. Burger, A. Ballin, E. Cutz, and A. C. Bryan. 1987. Effect of granulocyte depletion in a ventilated surfactant-depleted lung. *J. Appl. Physiol.* 62:27–33.
5. Parker, J. C., L. A. Hernandez, G. L. Longenecker, K. Peevy, and W. Johnson. 1990. Lung edema caused by high peak inspiratory pressure in dogs. *Am. Rev. Respir. Dis.* 142:321–328.
6. Webb, H. H., and D. F. Tierney. 1974. Experimental pulmonary edema due to intermittent positive pressure ventilation with high inflation pressures: protection by positive end-expiratory pressure. *Am. Rev. Respir. Dis.* 110:556–565.
7. Dreyfuss, D., and G. Saumon. 1993. Role of tidal volume, FRC, and end-inspiratory volume in the development of pulmonary edema following mechanical ventilation. *Am. Rev. Respir. Dis.* 148:1194–1203.
8. Crandall, E. D., and K.-J. Kim. 1991. Alveolar epithelial barrier properties. *In* R. G. Crystal and J. B. West, editors. The Lung: Scientific Foundations. Raven Press, New York. 273–287.
9. Matthay, M. A., and J. P. Wiener-Kronish. 1990. Intact epithelial barrier function is critical for resolution of alveolar edema in humans. *Am. Rev. Respir. Dis.* 142:1250–1257.
10. Tschumperlin, D. J., and S. S. Margulies. 1999. Alveolar epithelial surface area-volume relationship in isolated rat lungs. *J. Appl. Physiol.* 86:2026–2033.
11. Dreyfuss, D., P. Soler, G. Basset, and G. Saumon. 1988. High inflation pressure pulmonary edema. *Am. Rev. Respir. Dis.* 137:1159–1164.
12. Egan, E. A. 1980. Response of alveolar epithelial solute permeability to changes in lung inflation. *J. Appl. Physiol.* 49:1032–1036.
13. Egan, E. A. 1982. Lung inflation, lung solute permeability, and alveolar edema. *J. Appl. Physiol.* 53:121–152.
14. Egan, E. A., R. M. Nelson, and R. E. Olver. 1976. Lung inflation and alveolar permeability to non-electrolytes in the adult sheep *in vivo*. *J. Physiol. (Lond.)* 260:409–424.
15. Kim, K.-J., and E. D. Crandall. 1982. Effects of lung inflation on alveolar epithelial solute and water transport properties. *J. Appl. Physiol.* 52: 1498–1505.
16. Fu, Z., M. L. Costello, K. Tsukimoto, R. Prediletto, A. R. Elliott, O. Mathieu-Costello, and J. B. West. 1992. High lung volume increases stress failure in pulmonary capillaries. *J. Appl. Physiol.* 73:123–133.
17. Tschumperlin, D. J., and S. S. Margulies. 1998. Equibiaxial deformation-induced injury of alveolar epithelial cells *in vitro*. *Am. J. Physiol.* 275: L1173–L1183.
18. Parker, J. C., L. A. Hernandez, and K. J. Peevy. 1993. Mechanisms of ventilator-induced lung injury. *Crit. Care Med.* 21:131–143.
19. Dobbs, L. G., R. Gonzales, and M. C. Williams. 1988. An improved method for isolating type II cells in high yield and purity. *Am. Rev. Respir. Dis.* 134:141–145.
20. Mason, R. J., M. C. Williams, J. H. Widdicombe, M. J. Sanders, D. S. Misfeldt, and L. G. Berry, Jr. 1982. Transepithelial transport by pulmonary alveolar type II cells in primary culture. *Proc. Natl. Acad. Sci. U.S.A.* 79:6033–6037.
21. Paine, R., III, and R. H. Simon. 1996. Expanding the frontiers of lung biology through the creative use of alveolar epithelial cells in culture. *Am. J. Physiol.* 270:L484–L486.
22. Danto, S. I., S. M. Zabski, and E. D. Crandall. 1992. Reactivity of alveolar epithelial cells in primary culture with type I cell monoclonal antibody. *Am. J. Respir. Cell Mol. Biol.* 6:296–306.
23. Dobbs, L. G., M. C. Williams, and A. E. Brandt. 1985. Changes in biochemical characteristics and pattern of lectin binding of alveolar type II cells with time in culture. *Biochim. Biophys. Acta* 846:155–166.
24. Ellis, E. F., J. S. McKinney, K. A. Willoughby, S. Liang, and J. T. Povlishock. 1995. A new model for rapid stretch–induced injury of cells in

culture: characterization of the model using astrocytes. *J. Neurotrauma* 12:325–339.
25. Schneeberger, E. E. 1991. Alveolar type I cells. *In* R. G. Crystal and J. B. West, editors. The Lung: Scientific Foundations. Raven Press, New York. 229–234.
26. Cheek, J. M., K.-J. Kim, and E. D. Crandall. 1989. Tight monolayers of rat alveolar epithelial cells: bioelectric properties and active sodium transport. *Am. J. Physiol.* 256:C688–C693.
27. Tsuno, K., P. Prato, and T. Kolobow. 1990. Acute lung injury from mechanical ventilation at moderately high airway pressures. *J. Appl. Physiol.* 69:956–961.
28. Harris, J. B., L.-Y. Chang, and J. D. Crapo. 1991. Rat lung alveolar type I epithelial cell injury and response to hyperoxia. *Am. J. Respir. Cell Mol. Biol.* 4:115–125.
29. Berg, J. T., Z. Fu, E. C. Breen, H.-C. Tran, O. Mathieu-Costello, and J. B. West. 1997. High lung inflation increases mRNA levels of ECM components and growth factors in lung parenchyma. *J. Appl. Physiol.* 83:120–128.
30. Wirtz, H. R. W., and L. G. Dobbs. 1990. Calcium mobilization and exocytosis after one mechanical stretch of lung epithelial cells. *Science* 250:1266–1269.
31. Zhang, S., V. Garbutt, and J. T. McBride. 1996. Strain-induced growth of the immature lung. *J. Appl. Physiol.* 81:1471–1476.
32. Vejlstrup, N. G., C. A. R. Boyd, and K. L. Dorrington. 1994. Effect of lung inflation on active and passive liquid clearance from *in vivo* rabbit lung. *Am. J. Physiol.* 267:L482–L487.
33. Lecuona, E., F. Saldias, A. Comellas, K. Ridge, C. Guerrero, and J. I. Sznajder. 1999. Ventilator-associated lung injury decreases lung ability to clear edema in rats. *Am. J. Respir. Crit. Care Med.* 159:603–609.
34. Coker, P. J., L. A. Hernandez, K. J. Peevy, K. Adkins, and J. C. Parker. 1992. Increased sensitivity to mechanical ventilation after surfactant inactivation in young rabbit lungs. *Crit. Care Med.* 20:635–640.
35. Hernandez, L. A, P. J. Coker, S. May, A. L. Thompson, and J. C. Parker. 1990. Mechanical ventilation increases microvascular permeability in oleic acid-injured lungs. *J. Appl. Physiol.* 69:2057–2061.
36. Dambrosio, M., E. Roupie, J.-J. Mollet, M.-C. Anglade, N. Vasile, F. Lemaire, and L. Brochard. 1997. Effects of positive end-expiratory pressure and different tidal volumes on alveolar recruitment and hyperinflation. *Anesthesiology* 87:495–503.
37. Pelosi, P., L. D'Andrea, G. Vitale, A Pesenti, and L. Gattinoni. 1994. Vertical gradient of regional lung inflation in adult respiratory distress syndrome. *Am. J. Respir. Crit. Care Med.* 149:8–13.
38. Amato, M. B. P., C. S. V. Barbas, D. M. Medeiros, G. P. P. Schettino, G. L. Filho, R. A. Kairalla, D. Deheinzelin, C. Morais, E. O. Fernandes, T. Y. Takagaki, and C. R. R. Carvalho. 1995. Beneficial effects of the "open lung approach" with low distending pressures in acute respiratory distress syndrome. *Am. J. Respir. Crit. Care Med.* 152:1835–1846.